EFFECTS OF SURFACTANTS ON AQUEOUS FOAMS PROPERTIES: A STEP TOWARD MINERAL FOAMS

Nourhan Mortada[1,*], Annabelle Phelipot-Mardelé[1], Christophe Lanos[1]

Abstract

This study focus on foaming properties of three surfactants: α-olefin sulphonate sodium salt (Hostapur OSB), Trimethyl tetradecyl ammonium bromide (Cetrimide) and Hexadecyl trimethyl ammonium bromide (CTAB) usable for mineral foaming. The ability of these surfactants to reduce surface tension is evaluated. Foamability and foam stability of aqueous foams made up with these surfactants are assessed at different concentrations, using the Dynamic Foam Analyzer providing parameters which describe the foaming and decay phases. They considerably depend on the type of surfactant and its concentration. By analyzing the bubble size distribution, the relationship between the stability and the foam structure can be observed. The Hostapur OSB appears to be the most efficient surfactant in terms of stability and foamability, representing the thinnest foam structure and the highest characteristic times (deviation, transition and half-life) at CMC (critical micelle concentration).

Keywords: Foamability, stability, foam structure, surfactant, surface tension.

1. Introduction

European energy consumption continues to grow. The building sector appears as the largest consumer of energy, accounting for 46% of energy consumption, of which 50% is used for space heating and cooling [1, 2]. Heat loss through building walls remains the main cause of the high energy consumption. This sector accounts also for 25% of greenhouse gas emissions. In 2015, the European Union Emissions Trading [3] reported approximately 574 Mt of industrial greenhouse gas emissions. European emission reduction aims to reduce emissions in all sectors by at least 40% by 2030 and

* Corresponding author
Email address: nourhan.mortada@univ-rennes1.fr (Nourhan Mortada)
[1]Univ Rennes, LGCGM, 3 rue du Clos Courtel, BP 90422, 35704 Rennes, France.

80-95% by 2050 (carbon neutrality) compared to 1990 [4]. Thus, reducing the environmental impact of the building sector has become a key element of sustainable development.

The building sector must therefore optimize the energy performance of its buildings and promote new materials that comply with regulations in terms of environmental impact and the comfort of residents. In this perspective, innovation in terms of insulating and load-bearing materials is an important challenge. Current research includes bio-sourced composites and lightweight concrete. Various studies [5, 6, 7, 8] have been carried out on these two types of materials to determine their physical, mechanical and thermal characteristics. Over the past years, lightweight concrete has been developed with the aim of reducing the density of load-bearing materials, limiting the consumption of raw materials and obtaining better thermal performance than concrete and conventional insulation [9, 10, 11], such as mineral foams. The studies that have been conducted on the thermal performance of foamed concrete have shown that thermal conductivity is a linear function of the density (i.e. the porosity) of hardened mineral foams [12, 13]. The possibilities of using foam concrete have been extended thanks to its structural characteristics, combined with low density and low energy consumption for production. They are produced by inserting gas into a fresh paste of a mineral hydraulic binder through chemical or mechanical foaming. In order to obtain a stable foam and a durable dispersion of gas bubbles until hardening, foaming agents are essential. Due to their amphiphilic nature, these agents adsorb at the gas/fluid interfaces and change the interfacial rheology by reinforcing the viscoelastic character of interfaces due to the electrostatic repulsion [14, 15, 16, 17, 18, 19]. The hydrophilic part of these agents is placed in the water while the hydrophobic part is placed in the air. By adsorbing in this way, the surfactants form a monomolecular film and reduce surface tension. From a certain surfactant concentration in water, called critical micellar concentration (CMC), the surface at the interface becomes saturated with surfactant molecules. Over the CMC, the surface tension no longer changes and excess of surfactant forms micelles [20]. CMC is often used as the optimal concentration to create stable aqueous foams.

The significant evolution of the structure of foams over time makes it difficult to describe their geometry [21]. It varies under the effect of physical parameters such as liquid volume fraction, bubble size, fluid viscosity, temperature and pressure, and

under the effect of physical-chemical parameters such as surface tension, surfactant adsorption and interfacial rheology. During time, liquid drainage phenomena can occur. It corresponds to the flow of water contained in foams under the influence of gravity. This causes the foam drying, a change in the concentration of surfactants, and therefore the rupture of liquid films leading to the coalescence of adjacent bubbles. In addition, air in small bubbles tend to diffuse into large bubbles due to the difference in internal gas pressures; this phenomenon is called coarsening. These three phenomena, drainage-coalescence-coarsening lead to a decrease in the number of bubbles and an increase in their average size over time [16, 17, 18, 19, 21].

This study is the first step in a larger research to understand how the structure of aqueous foam interacts with the structure and the final porosity of mineral foam. Assuming the fresh mineral foam as an aqueous foam in mix with concentrated suspension, the mineral foam stability is conditioned by aqueous foam stability. Therefore, in this paper we investigate the effect of three commercial formulated surfactants used for mineral foams (Hostapur OSB, CTAB and Cetrimide) on the foamability and porous structure (stability) of aqueous foams. At first, the ability of surfactants to reduce surface tension is measured. The CMC of each surfactant is also determined based on the surface tension isotherm. The foamability results obtained at the CMC are then discussed and their effect on the stability and porous structure of aqueous foams are evaluated. The observation of the bubble size and their distribution over time allows us comparing the effect of each surfactant on the decay process. Based on these results, a classification and qualification of the best surfactant is sought.

2. Materials

As explained, agitating the pure water without any addition generates bubbles that disappear quickly due to the rapid liquid drainage followed by coalescence and coarsening. The addition of foaming agents is therefore necessary to stabilize the water films and to have a stable foam. Three different agents successfully tested for the production of gypsum based mineral foams [12] or super sulfated cement foams [22] are selected: Hostapur OSB from Clariant Produkte®, CTAB and Cetrimide from Novo Nordisk Pharmatech A/S®. Their type and chemical composition are shown in Table 1.

Table 1: Surfactants characteristics

Surfactant	Type	Chemical formula	Producer
Hostapur OSB	Anionic	$C14_{/16}$:*α-olefin* sulphonate sodium salt	Clariant Produkte
CTAB	Cationic	C19H42NBr: Hexadecyl trimethyl ammonium bromide	Novo Nordisk Pharmatech A/S
Cetrimide	Cationic	C17H38NBr: Trimethyl tetradecyl ammonium bromide	Novo Nordisk Pharmatech A/S

3. Methods

3.1. Tensiometer

Surface tension at the interface between air and aqueous solution of each surfactant was measured with a KRUSS "Drop Shape Analyser DSA30" tensiometer as depicted in Figure 1 (left). Tests were made at ambient conditions: T = 23±1 °C and HR = 60%, using the pendant drop method as shown in Figure 1 (right). The drops are produced using a 15 gauge needle, with an external diameter of 1.835 mm. The drop appears with a flow of 0.2 $\mu l/s$ and manually controlled volume. In the process, the instrument digitally record and analyzes the shape of the drops formed at the tip of the syringe. The injection was stopped when the shape of the drop was clearly detached from the straight tip of the needle as can be seen in Figure 1 (right). The surface tension is obtained with a resolution of 0.01 mN/m, from an analysis of the shape of the drop by balancing the internal and external forces acting on the drop and based on the Young-Laplace equation. The reported surface tension values are the average of at least 20 measurements (10 measurements/drop). Surface tension of distilled water was measured at ambient conditions. An average absolute deviation of 0.29% was obtained between experimental data (γ_{water} = 72.96mN/m) and references data (γ_{water} = 72.75 mN/m) [23] at 20 °C.

In order to determine the CMC of each surfactant in water, several tests were conducted to plot the surface tension curve as a function of the surfactant concentration. An initial solution with a concentration of 7966 ± 1 mg/l was prepared

for each surfactant with distilled water. By dilution, a concentration range from 200 to 7966 *mg/l* was reached using a concentration step of 0.1 in logarithmic scale.

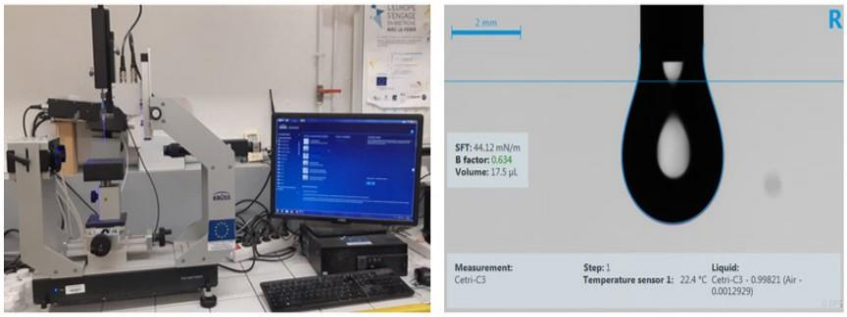

Figure 1: Equipment of the Tensiometer DSA30 (left). Example of pendant drop image of a Cetrimide solution (right)

3.2. Dynamic Foam Analyzer

The Dynamic Foam Analyzer DFA100 from KRUSS is used in our study to measure foamability, foam stability and structure produced with each surfactant solutions. As shown in Figure 2, the device is equipped with several photon detectors allowing the analysis of the intensity of the light, passing through the foamed solution and diffused by a LED panel placed throughout the test column as shown in Figure 2 (left). As both gas and liquid are translucent, the two interfaces liquid/foam and foam/gas are detected using the difference between the measured light intensity values. The software then deduces the heights of the liquid and foamed part over time. For all measurements, 50 *ml* of surfactant solution is placed with a syringe into a transparent glass column of 44 *mm* inner diameter, placed between the LED panel and the optical sensors (Photon detector). For foaming, the compressed air is injected through a porous stone placed on the base of the column, using an external pump at a gas flow of 0.3 *l/min* for 18 *s*. The pore sizes of this stone range between 40 and 100 μm.

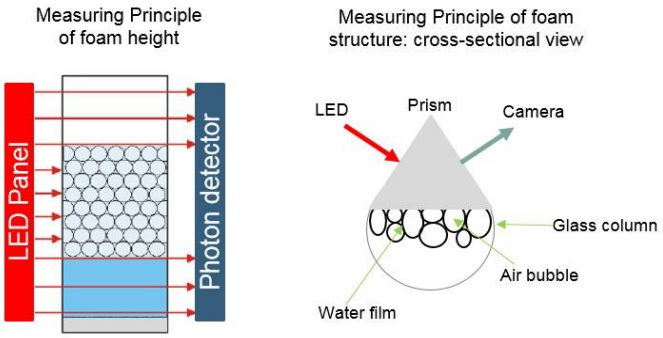

Figure 2: Concept of foam height and structure measurements [24]

The Foam Structure Module allows the measurements of the 2-dimensional foam structure. As described previously, the foam is generated in a glass column equipped with a prism integrated over the entire height of the column as depicted in Figure 2 (right). According to the principle of total reflection, this prism generates images of the bi-dimensional foam structure with high contrast. The high-contrast images detected by the camera are analyzed with the foam analyzer software. This analysis gives the bubble size and number distributions and its evolution during time. Figure 3 shows an example of distributions of bubble number and size based on a photo recorded 10 min after the end of foaming. Knowing that the foam dries quickly in the upper part and remains wet in the lower part, the choice to place the camera in the middle (at 70 *mm* above the porous stone) seems to be the optimal position to observe the bubble size during the entire life of the foam.

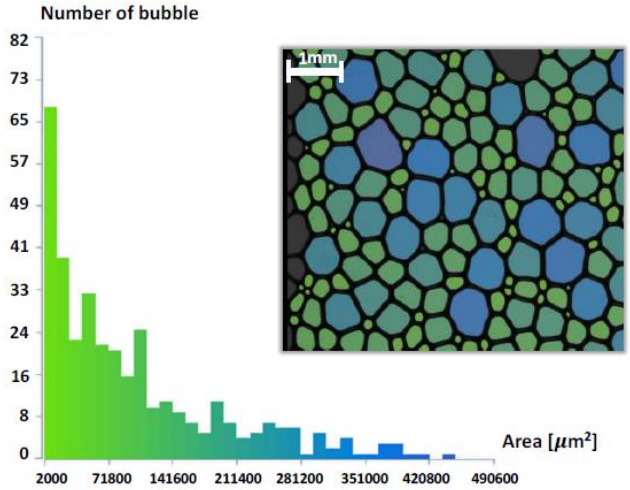

Figure 3: Bubble number distribution as a function of the area μm^2 for the Hostapur OSB foam, produced with a concentration equal to the CMC, recorded 10 min after the end of foaming.

4. Results and Discussions

4.1. Surface tension and CMC of surfactants

Figure 4 shows the evolution of surface tension versus concentration of the three surfactants. Surface tension values are determined by averaging 20 measurements per concentration. The shape of the obtained curve corresponds to the one of the surface tension isotherm derived from Gibbs equation [25, 26].

The rupture of the slope in the curve allows us to determine the CMC (Figure 4). The CMC of Hostapur OSB is 796 *mg/l*. This concentration corresponds to a surface tension γ_{OSB} = 35.69 ± 0.5 *mN/m*. Cetrimide and CTAB belong to the same cationic family of surfactants; they also have a similar chemical composition. This explains the close values of associated surface tension with CMC: γ_{CTAB} = 37.19 ± 0.18 *mN/m* and $\gamma_{Cetrimide}$ = 38.14 ± 0.21 *mN/m*. These values agree with Samson's et al, values [27]. However, these two surfactants present different CMC: CMC_{CTAB} = 358*mg/l* (0.982*mM*) and $CMC_{Cetrimide}$ = 1261 *mg/l* (3.75 *mM*). These results are also coherent with those obtained in the literature [27, 28, 29].

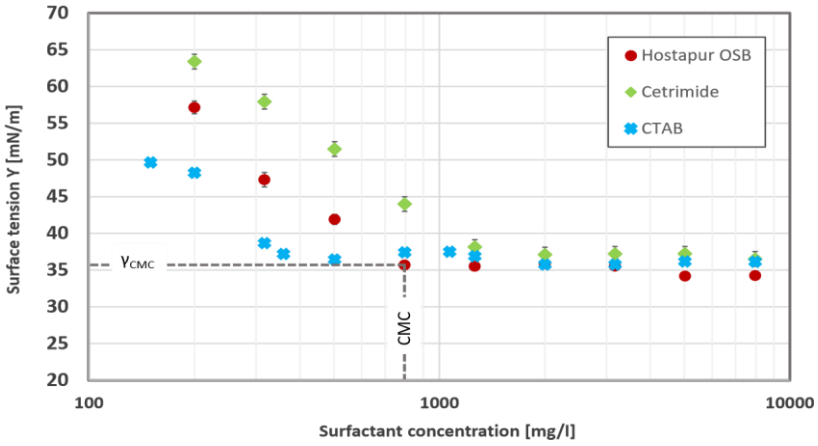

Figure 4: CMC evaluation of the three tested surfactants.

4.2. Foamability and foam stability

For each surfactant, the foamability and the foam stability are studied using the results of DFA tests. The measurements give the evolution of the total height of the

aqueous foam as a function of time. The total height is the sum of the foam height and the liquid height, data also provided by the device (Figure 5). In Figure 5, the device creates the foam from 0 s to t_0. t_0 indicates the end of foaming when the total height correspond to a maximum: h_{max}; after, the foam destruction begins. Lunkheimer and Malysa [30] divided this foam destruction into three phases starting from the initial point t_0:

- During the first phase, the liquid drainage process begins, but the total height remains constant as the quantity of liquid drained compensates the quantity of decayed foam. The end of this phase is remarked by t_{dev} (deviation time), which delineates the initial decrease of the total height.

- The second phase, begining at t_{dev}, is called the destructive phase where the total height decreases due to the foam decay associated to liquid drainage. This phase ends with t_{tr} corresponding to the time where the drainage is completed.

- The third phase begins at t_{tr} which can be detected once the liquid height under the foam remains constant and the foam is quite dry.

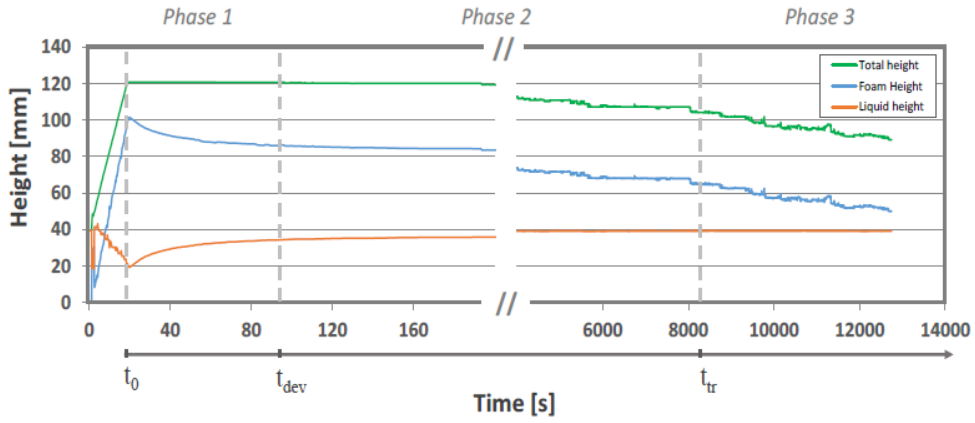

Figure 5: Measuring total height, foam height and solution (liquid) height versus time - Hostapur OSB foam at CMC.

The foamability of surfactants can be directly correlated with the Total height created after the end of bubbling at t_0. Foam stability can be characterized and studied through its slow destruction in time. t_{dev} is one of the stability criteria, so that only the

beginning of phases 1 and 2 is considered for all foams. The other parameter characterizing the stability of foams is the half-life time $t_{50\%}$. This time represents the moment when the foam height is reduced by half, compared to the initial foam height at t_0.

In order to determine the surfactant concentration at which foamability is considered optimal, three concentrations were studied as shown in the Table 2. It should be noted that for CTAB concentration equal to 0.1 CMC and Cetrimide concentration equal to 0.5 and 0.1 CMC, the foam formation is not possible with the chosen flow rate of 0.3 *l/min*. With a concentration equal to 2 CMC, Cetrimide presents good foamability despite the low flow rate, however the foam appears unstable in the long term (less half-life time).

Table 2: Surfactants concentrations studied for foamability and stability.

Surfactants	Hostapur OSB			Cetrimide				CTAB		
CMC	796 *mg/l*			1261 *mg/l*				358 *mg/l*		
Content/CMC	0,1	0,5	1	0,1	0,5	1	2	0,1	0,5	1
Concentration [mg/l]	80	398	796	126	631	1261	2524	36	179	358
Number of trials	3	7	7	3	5	5	4	3	4	7
Foamibility	Yes	Yes	Yes	No	Yes	Yes	Yes	No	No	Yes
Half-Life time [s]	1445	10522	12328	-	564	3200	2493	-	-	6000

The foaming results with a concentration equal to CMC are presented in Figure 6 (left) and in Table 4. Three different resting times: t_0, 1000 *s* and 3000 *s* allow to sort through the data and highlight the evolution of the structure of the foams over time (Figure 6 (right)). The foamed part of the solution at t_0 is more than twice the initial height of the solution (32.88 *mm* for 50 *ml*); so all three surfactants present good foamability at CMC. Hostapur OSB generates a foam height of 102.75 *mm*, which is higher than the height obtained with Cetrimide 100.35 *mm* and with CTAB 89.7 *mm*, as shown in the right panel of Figure 6 and in the zoomed part in the left panel. These curves correspond properly to the different phases presented above. The stability difference between the three foams is represented by the shapes of the decay curves. Despite the good foamability of all three surfactants at CMC, the stability of foams differs. The curves of Hostapur OSB and CTAB present a good linearity over time, the slope being more significant for CTAB, indicating a lower stability. Conversely, the foam formed with Cetrimide decomposes in different ways, with a first slope similar to

CTAB and a second one more significant and stronger, leading to the lowest stability of the three surfactants. Based on the foamability values before 1000 *s*, a first classification of surfactants can be considered: Hostapur OSB is the best surfactant, followed by Cetrimide and then CTAB. This classification is preliminary, as it is based purely on foamability at CMC. Foams obtained with Hostapur OSB and CTAB are more stable and decay more slowly.

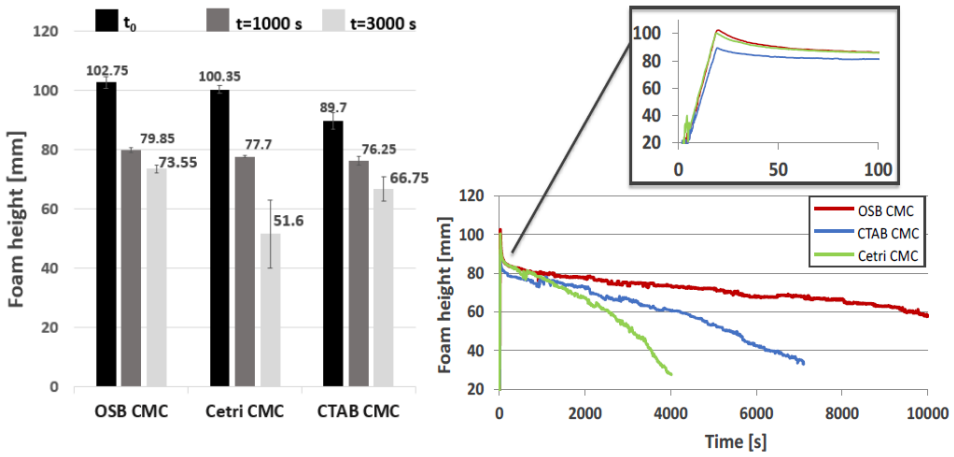

Figure 6: Left: The foam height at t_0, t = 1000 s and t = 3000 s. Right: Time dependence of the foam height for three formed foams (zoom: during the first 100 s of height measurements).

After t_0, foams proceed to the first phase of destruction where the drainage is associated with film rupture and thus a decrease in the foam height. The difference ($\Delta H_F - \Delta H_L$) between the foam height H_F and the liquid height H_L from t_0, versus time allows to determine t_{dev} according to Lunkheimer and Malysa [31]. The shapes of obtained curves (Figure 7) are similar to those presented by these authors. The most stable foam is that obtained with Hostapur OSB, followed by CTAB and Cetrimide with a deviation time of 77 *s*, 60 *s* and 45 *s* respectively (Table 3).

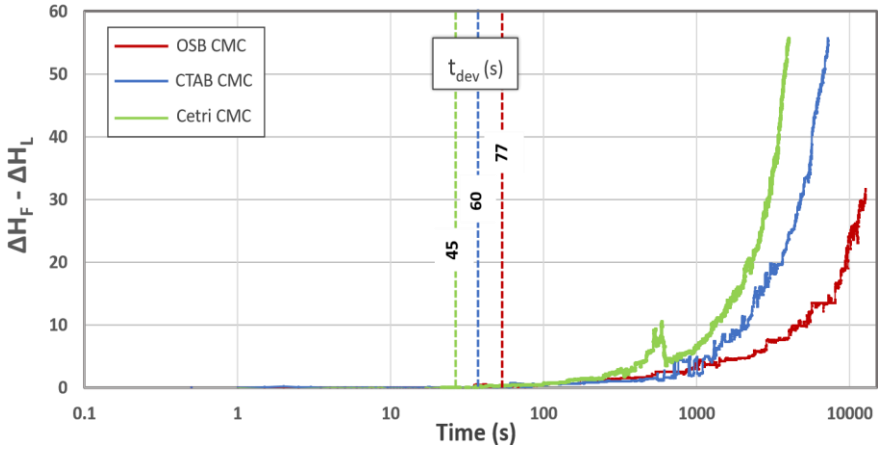

Figure 7: Evolution of $\Delta H_F - \Delta H_L$ in time for Hostapur OSB, CTAB and Cetrimide at CMC. $\Delta H_F - \Delta H_L$: the difference between the foam height and the liquid height from t_0.

The $t_{50\%}$ values of these foams are shown in Table 2, it is reasonable to expect that Hostapur has the largest $t_{50\%}$ (12328 *s*) considering the results previously analyzed. The CTAB presents a $t_{50\%}$ of 6000 *s* twice as long as Cetrimide's 3200 *s*. This difference between these two cationic surfactants can be explained by the chains length since a higher length insure more stability [32]. More, in the case of Cetrimide, a concentration equal to 2CMC allows to have more foam but a less half-life time (Table 2). Such results call for fixing the concentration to the CMC.

In view of all these results, the proposed classification by simply studying foamability is no longer valid. Although Cetrimide has a greater foamability than CTAB, it is not sufficiently effective in terms of stability. A classification of surfactant in terms of foamability and stability at CMC can be proposed as follows: Hostapur OSB followed by CTAB and Cetrimide.

Between t_0 and $t_0 + t_{dev}$ the aqueous foam stability can be studied by analysing the volume of water associated to the foam, acting as a good indication of the foam density. According to the size of the bubble and the surface tension, the foam density conditions the gas pressure level imposed into the bubbles. The ratio of the liquid volume and aqueous foam V_W/V_F obtained at t_0 and t_{dev} are detailed in Table 3. At CMC, CTAB leads to a driest foam than the other surfactants. Hostapur OSB and Cetrimide present a quite similar waterin-foam ratio, but the end of phase 1 occurs faster for Cetrimide than Hostapur OSB. A concentration higher than the CMC doesn't affect significantly V_W/V_F ratio but increases the phase 1 duration (Cetrimide example shown in the Table 3). For

a concentration below the CMC, aqueous foam density of Cetrimide is more penalized than that of Hostapur OSB and phase 1 is shortened. These results confirms once again the greater robustness of Hostapur OSB.

Table 3: Ratio of liquid volume V_W and aqueous foam V_F, at t_0 and t_{dev}.

Surfactants	Hostapur OSB		Cetrimide			CTAB	
Content/CMC	0,5	1	0,5	1	2	0,5	1
V_W/V_F at t_0	0,181	0,195	0,102	0,182	0,2	-	0,107
V_W/V_F at t_{dev}	0,119	0,055	0,078	0,064	0,047	-	0,035
t_{dev} [s]	20	77	6	45	118	-	60

4.3. Foam structure

By analyzing the foam structure, it is possible to see the bubble distribution in size and to deduce many parameters such as the mean of the radius (r_{mean}) and the Sauter radius (r_{32}). It is thus possible to compare these parameters over time and then determine the effect of surfactants on foam structure. Results of foams formed at a concentration equal to the CMC are presented in this section.

From t_0 to t_{dev}, aqueous foam here defined as the bubbles and water needed for their formation, is considered to be stable. After the end of the bubbling, 20 seconds are needed to drain the excess of water trapped in the part of the foam above the camera and eliminate any effect of the bubbling step dynamics. This time is chosen as an initial reference for the analyses of the foam structure, named t_{stab}. Figure 8 shows the structure of foams formed with the three surfactants at t_{stab}, 1000 *s* and 3000 *s*. The objective is to record the evolution of the structure of the foams over time. The images show that at t_{stab}, the foam created with Hostapur OSB has a slightly finer structure than with Cetrimide. Both foams have a finer distribution than CTAB. At 1000 *s*, the evolution of structures shows a different trend: Hostapur OSB has still the finest structure, but Cetrimide has now the structure with the biggest bubbles. After 3000 *s*, foams formed with Hostapur OSB presents always the finest distribution compared to the other two foams. The poral structure appears coarser for the CTAB foam. The Cetrimide foam presents a poral structure with the largest bubbles. These observations show that Cetrimide foam evolves more than Hostapur OSB and CTAB, coalescence is more important.

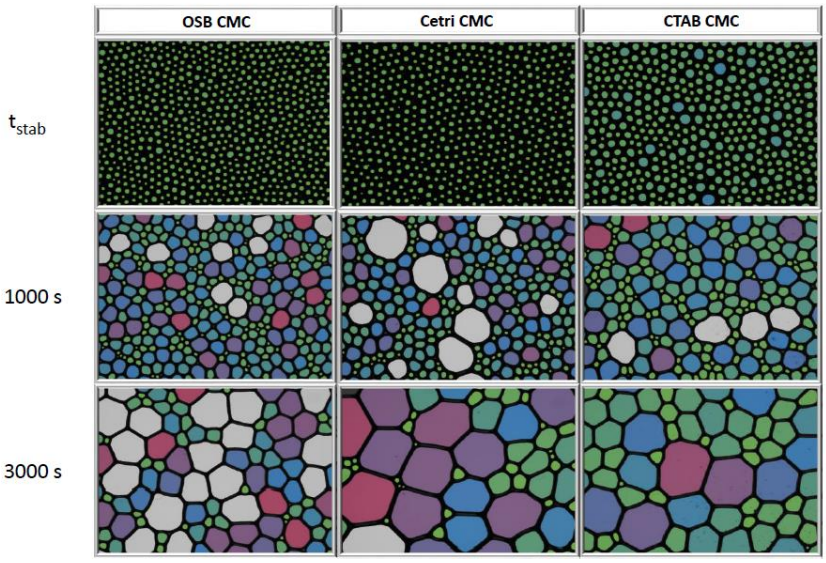

Figure 8: Images showing the evolution of the foams structure formed with three surfactants over time.

For each foam, the bubbles area evaluated from visualizations are classified into different ranges. The area of each bubble is used to calculate the radius of equivalent circular surface. These values allow to calculate the surface proportions of each class and finally to evaluate the alveolar distribution: frequency and cumulative (Figure 9). At t_{stab}, the frequency alveolar distribution shows that the three foams have a monodisperse size distribution. The curves are close and results are in accordance with the images presented in Figure 8. The Hostapur OSB and Cetrimide foams show a thinner structure than the CTAB. After 3000 *s*, these curves show a noticeable evolution. The alveolar distributions become more flat, indicating an increase in bubble size. The structure of Hostapur OSB and CTAB foams appear somewhat monodisperse, with larger bubbles. Cetrimide foam has a polydisperse size distribution. These observations are explained by the phenomenon of coalescence and coarsening.

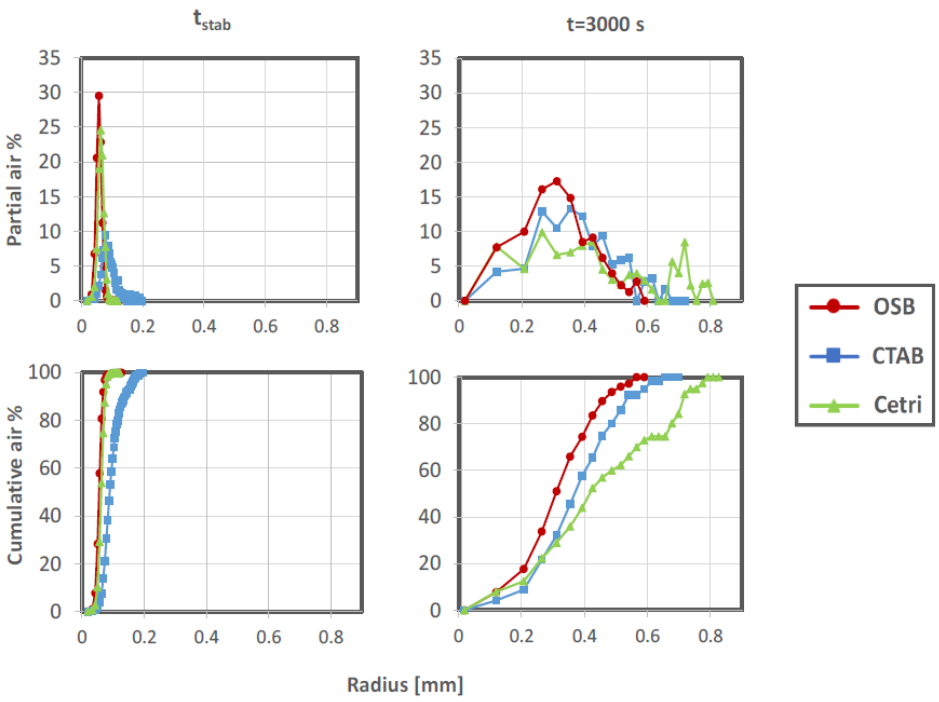

Figure 9: Frequency and cumulative alveolar distribution of the three aqueous foams formed at CMC.

It is also possible to calculate the Sauter mean radii r_{32} as given in equation (1). This parameter represents the mean radius of the bubbles present on the studied surface calculated from the Volume/Surface ratio of each bubble, which is different from the mean radius (r_{mean}) calculated from the area of each bubble (equation (2)). For the calculus, the volume of each bubble is assumed equal to r^3 and the surface equal to r^2. The polydispersity of bubble size distribution is evaluated using a polydispersity index PI as shown in (2):

$$r_{32} = \frac{\sum_{i=1}^{n} r_i^3}{\sum_{i=1}^{n} r_i^2} \quad (1)$$

$$PI = \frac{\sqrt{\bar{r^2} - (r_{mean})^2}}{r_{mean}} \quad \text{With :} \quad \bar{r^2} = \frac{\sum_{i=1}^{n} r_i^2}{n} \quad \text{and} \quad r_{mean} = \frac{\sum_{i=1}^{n} r_i}{n} \quad (2)$$

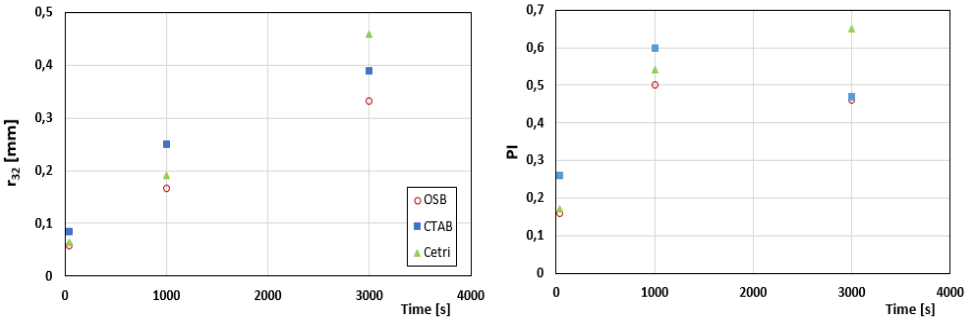

Figure 10: Comparison of r_{32} [mm] values (left) and PI values (right) at t_{stab}, 1000 *s* and 3000 *s*.

Values of Sauter radii and polydispersity index are summarized in Figure 10 at t_{stab}, 1000 *s* and 3000 *s*. In all cases, the parameters significantly increase with time. Hostapur OSB still has the finest distribution (r_{32} and PI minimum values) compared to the other two surfactants. At t_{stab}, the calculated Sauter radii for the three surfactants Hostapur OSB, Cetrimide and CTAB are 0.059, 0.065 and 0.084 *mm* respectively. The polydispersity index of Hostapur OSB and Cetrimide foams are very similar: 0.16 and 0.17 respectively. These two values are lower than the one obtained for CTAB foam: 0.26 as shown in Figure 10 (right). After 3000 *s*, for Hostapur OSB, the Sauter radius increased from 0.059 to 0.33 *mm* with a PI of 0.46. This increase reflects very well the bubbles coalescence observed in the images of the porous structures in Figure 8 at t_{stab} and 3000 *s*. These different parameters values are summarized in Table 4.

The foam structure obtained with CTAB appears to be somewhat monodispersed after 3000 *s*, with a PI of 0.49 *mm*. Cetrimide foam has a polydispersed structure as shown in Figure 8 with a PI of 0.65 *mm* and with the biggest bubbles r_{32} = 0.46 *mm*. These values show that Cetrimide foam evolves more than Hostapur OSB and CTAB foams: coalescence is more intense. Taking into account that t_{tr} = 2636 *s* for Cetrimide, the results at 3000 *s* are in phase 3, unlike the other two surfactants. These results are in accordance with those presented previously regarding the foamability and stability. Curiously, the PI values at 1000 *s* for OSB and CTAB are higher than those at t_{stab} and 3000 *s*, showing somehow the incidence of coarsening.

Table 4: Structural and stability characteristics of studied foams at CMC.

Surfactants		Hostapur OSB	Cetrimide	CTAB
CMC [mg/l]		796	1261	358
Surface tension [mN/m]		35.69 ± 0,5	38.14 ± 0,21	37.18 ± 0,18
at tstab	Foam hieght [mm]	100.35	102.75	89.7
	r32 [mm]	0.059	0.065	0.084
	PI	0.16	0.17	0.26
at 1000 s	Foam hieght [mm]	79.85	77.7	76.25
	r32 [mm]	0.16	0.19	0.25
	PI	0.48	0.54	0.6
at 3000 s	Foam hieght [mm]	73.55	51.6	66.75
	r32 [mm]	0.33	0.46	0.39
	PI	0.46	0.65	0.49
tdev [s]		77	45	60
ttr [s]		8480	2636	3812
$t50_{\%}$ [s]		12328	3200	6000

5. Conclusion

The ability of three surfactants, Hostapur OSB, CTAB and Cetrimide, to reduce surface tension of aqueous solution is evaluated using a tensiometer. Quite the same surface tensions are obtained at the critical micellar concentration of each surfactant. A foam analyzer is used to analyze the foamability of these surfactants and the stability of aqueous foams formed with various surfactant concentrations. In the same test conditions, at the critical micellar concentration of each surfactant, the foamability expressed by the obtained foam density appears quite equivalent (V_W/V_F equal) for Hostapur OSB and Cetrimide. The CTAB foam appears drier. However, the kinetic of water percolation into the foam differs. For same initial aqueous foam density, shorter t_{dev} indicates lower stability. Interestingly, above a sufficient concentration, increasing the surfactant concentration (until 2CMC) doesn't affect the ratio of water trapped in the aqueous foam but only changes the produced foam volume and consequently affects its stability, increasing t_{dev} but reducing $t_{50\%}$. The concentration equal to the CMC allows to have an optimum combining foaming power and stability. By analyzing

the aqueous foam structure, we can highlight the relationship between the evolution of the porous structure of foams and the type of surfactant. The foams formed with Hostapur OSB have the thinnest structure. CTAB foam structure presents the largest bubbles but with a monodispersed size distribution. The one with Cetrimide has small bubbles but a polydispersed size distribution. Structure modification versus time presents similar evolution for all the surfactants. A classification of surfactant efficiency is derived from the analysis: Hostapur OSB appears to be the most potent, followed by CTAB and Cetrimide. These results are a step toward mineral foams. Using these surfactants, gypsum and lime foams will be produced with different concentrations in order to produce lightweight material with insulating and moisture regulating properties.

Declaration of competing interest

The authors declare that they have no known competing financial interests or personal relationships that could have appeared to influence the work reported in this paper.

Data availability

The data that support the findings of this study are available from the corresponding author upon reasonable request.

References

[1] G. Zheng, Y. Jing, H. Huang, Y. Gao, Application of improved grey relational projection method to evaluate sustainable building envelope performance, Applied Energy 87 (2) (2010) 710–720. doi:10.1016/j.apenergy. 2009.08.020.

[2] M. Ozel, Thermal performance and optimum insulation thickness of building walls with different structure materials, Applied Thermal Engineering 31 (17) (2011) 3854–3863. doi:10.1016/j.applthermaleng.2011. 07.033.

[3] W. Eichhammer, A. Herbst, M. Pfaff, T. Fleiter, et B. Pfluger, *Impact on the environment and the economy of technological innovations for the Innovation Fund*

(IF) : in the fields of : energy-intensive industries, renewables, carbon capture and storage / use (CCS/CCU), energy storage. 2018.

[4] R. Pachauri, L. Meyer, et R. Myles, « IPCC 2014: Climate Change 2014: Synthesis Report. Contribution of Working Groups I, II and III to the Fifth Assessment Report of the Intergovernmental Panel on Climate Change (IPCC) », IPCC, Geneva, Switzerland, 2014.

[5] K. Ramamurthy, E. Kunhanandan Nambiar, G. Indu Siva Ranjani, A classification of studies on properties of foam concrete, Cement and Concrete Composites 31 (6) (2009) 388–396. doi:10.1016/j.cemconcomp.2009.04. 006.

[6] B. Chen, N. Liu, A novel lightweight concrete-fabrication and its thermal and mechanical properties, Construction and Building Materials 44 (2013) 691–698. doi:10.1016/j.conbuildmat.2013.03.091.

[7] S. Amziane, F. Collet, Bio-aggregates Based Building Materials: State-ofthe-Art Report of the RILEM Technical Committee 236-BBM, Springer, 2017.

[8] A. Çolak, Density and strength characteristics of foamed gypsum, Cement and Concrete Composites 22 (3) (2000) 193–200. doi:10.1016/ S0958-9465(00)00008-1.

[9] A. 122R-02, Guide to Thermal Properties of Concrete and Masonry Systems, ACI Committee Reports (2002).

[10] A. 213R-14, Guide for Structural Lightweight-Aggregate Concrete, ACI Committee Reports (2003).

[11] G. Samson, A. Phelipot-Mardelé, C. Lanos, A review of thermomechanical properties of lightweight concrete, Magazine of Concrete Research 69 (4) (2017) 201–216. doi:10.1680/jmacr.16.00324.

[12] G. Samson, A. Phelipot-Mardelé, C. Lanos, Thermal and mechanical properties of gypsum–cement foam concrete: effects of surfactant, European Journal of Environmental and Civil Engineering 21 (12) (2017) 1502–1521. doi:10.1080/19648189.2016.1177601.

[13] D. Aldridge, Introduction to foamed concrete: What, Why, How, in: Use of Foamed Concrete in Construction, Conference Proceedings, Thomas Telford Publishing, 2005, pp. 1–14. doi:10.1680/uofcic.34068.0001.

[14] V. Bergeron, D. Langevin, A. Asnacios, Thin-Film Forces in Foam Films Containing Anionic Polyelectrolyte and Charged Surfactants, Langmuir 12 (6) (1996) 1550–1556. doi:10.1021/la950654z.

[15] A. Asnacios, A. Espert, A. Colin, D. Langevin, Structural Forces in Thin Films Made from Polyelectrolyte Solutions, Phys. Rev. Lett. 78 (26) (1997) 4974–4977. doi:10.1103/PhysRevLett.78.4974.

[16] S. Hutzler, D. Weaire, Foam coarsening under forced drainage, Philosophical Magazine Letters 80 (6) (2000) 419–425. doi:10.1080/ 095008300403567.

[17] S. A. Koehler, S. Hilgenfeldt, H. A. Stone, A Generalized View of Foam Drainage: Experiment and Theory, Langmuir 16 (15) (2000) 6327–6341. doi:10.1021/la9913147.

[18] P. Stevenson, Foam Engineering: Fundamentals and Applications, John Wiley & Sons, 2012.

[19] I. Cantat, S. Cohen-Addad, F. Elias, F. Graner, R. H¨ohler, O. Pitois, F. Rouyer, A. Saint-Jalmes, Foams: Structure and Dynamics, OUP Oxford, 2013.

[20] R. K. Prud'homme, S. A. Khan, Foams: Theory, Measurements, and Applications, Vol. 57 of Surfactant Science series, Marcel Dekker, New York, 1997.

[21] D. L. Weaire, S. Hutzler, The Physics of Foams, Clarendon Press, Oxford, 1999.

[22] A. Phelipot-Mardelé, C. Lanos, G. Samson, C. Baux, Mineral Foams Obtained with Super Sulfated Cement, Key Engineering Materials 617 (2014) 36–39. doi:10.4028/www.scientific.net/KEM.617.36.

[23] N. B. Vargaftik, B. N. Volkov, L. D. Voljak, International Tables of the Surface Tension of Water, Journal of Physical and Chemical Reference Data 12 (3) (1983) 817–820. doi:10.1063/1.555688.

[24] Dynamic Foam Analyzer – DFA100, www.Kruss.de.

[25] J. W. Gibbs, Elementary principles in statistical mechanics: developed with especial reference to the rational foundation of thermodynamics, C. Scribner's sons, 1902.

[26] J. W. Gibbs, The collected works of J. Willard Gibbs., Tech. rep., Yale Univ. Press, (1948).

[27] G. Samson, Synthèse et propriétés des mousses minérales, Thesis, INSA Rennes, France (2015).

[28] J. Goronja, A. Janosevic-Lezaic, B. Dimitrijevic, A. Malenovic, D. Stanisavljev, N. Pejic, Determination of critical micelle concentration of cetyltrimethylammonium bromide: Different procedures for analysis of experimental data, Hemijska industrija 70 (4) (2016) 485–492. doi:10.2298/HEMIND150622055G.

[29] A. Dominguez, A. Fernandez, N. Gonzalez, E. Iglesias, L. Montenegro, Determination of Critical Micelle Concentration of Some Surfactants by Three Techniques, J. Chem. Educ. 74 (10) (1997) 1227. doi:10.1021/ ed074p1227.

[30] K. Lunkenheimer, K. Malysa, A simple automated method of quantitative characterization of foam behaviour, Polymer International 52 (4) (2003) 536–541. doi:10.1002/pi.1105.

[31] K. Lunkenheimer, K. Malysa, K. Winsel, K. Geggel, S. Siegel, Novel Method and Parameters for Testing and Characterization of Foam Stability, Langmuir 26 (6) (2010) 3883–3888. doi:10.1021/la9035002.

[32] C. Stubenrauch, K. Khristov, Foams and foam films stabilized by C_nTAB: Influence of the chain length and of impurities, Journal of Colloid and Interface Science 286 (2) (2005) 710–718. doi:10.1016/j.jcis.2005.01.107.